

New optical probes for the continuous monitoring of renal function

Richard B. Dorshow, Bethel Asmelash, Lori K. Chinen, Martin P. Debreczeny, Richard M. Fitch, John N. Freskos, Karen P. Galen, Kimberly R. Gaston, Timothy A. Marzan, Amruta R. Poreddy, Raghavan Rajagopalan, Jeng-Jong Shieh, William L. Neumann, Covidien, Imaging Solutions Research and Development, 675 McDonnell Blvd., Hazelwood, Missouri 63042

ABSTRACT

The ability to continuously monitor renal function via the glomerular filtration rate (GFR) in the clinic is currently an unmet medical need. To address this need we have developed a new series of hydrophilic fluorescent probes designed to clear via glomerular filtration for use as real time optical monitoring agents at the bedside. The ideal molecule should be freely filtered via the glomerular filtration barrier and be neither reabsorbed nor secreted by the renal tubule. In addition, we have hypothesized that a low volume of distribution into the interstitial space could also be advantageous. Our primary molecular design strategy employs a very small pyrazine-based fluorophore as the core unit. Modular chemistry for functionalizing these systems for optimal pharmacokinetics (PK) and photophysical properties have been developed. Structure-activity relationship (SAR) and pharmacokinetic (PK) studies involving hydrophilic pyrazine analogues incorporating polyethylene glycol (PEG), carbohydrate, amino acid and peptide functionality have been a focus of this work. Secondary design strategies for minimizing distribution into the interstitium while maintaining glomerular filtration include enhancing molecular volume through PEG substitution. *In vivo* optical monitoring experiments with advanced candidates have been correlated with plasma PK for measurement of clearance and hence GFR.

Keywords: Glomerular Filtration Rate, PEG, pyrazine, fluorescence, optical monitoring, clearance agents.

1. INTRODUCTION

Dynamic monitoring of renal function in patients at the bedside is highly desirable in order to minimize the risk of acute renal failure brought on by various clinical, physiological and pathological conditions.¹⁻⁵ It is particularly important in the case of critically ill or injured patients because a large percentage of these patients face the risk of multiple organ failure (MOF) resulting in death.^{6,7} MOF is a sequential failing of lung, liver, and kidneys and is incited by one or more severe causes such as acute lung injury (ALI), adult respiratory distress syndrome (ARDS), hypermetabolism, hypotension, persistent inflammation, or sepsis. The common histological features of hypotension and shock leading to MOF include tissue necrosis, vascular congestion, interstitial and cellular edema, hemorrhage, and microthrombi. These changes affect the lung, liver, kidneys, intestine, adrenal glands, brain and pancreas (in descending order of frequency).⁸ The transition from early stages of trauma to clinical MOF is marked by the extent of liver and renal failure and a change in mortality risk from about 30% to about 50%.⁹

In order to assess the status and to follow the progress of renal disease, there is a considerable interest in developing a simple, accurate, and continuous method for the determination of renal function, preferably by non-invasive procedures.¹⁰ Serum creatinine concentration measured at frequent intervals over a 24-hour period is currently the most common method of assessing renal function.^{11,12} The results from this analysis are frequently misleading since the value is affected by age, state of hydration, renal perfusion, muscle mass, dietary intake, and many other anthropometric and clinical variables. To compensate for these variances, a series of creatinine-based equations (most recently extended to cystatin C) have been developed which take into account sex, race and other factors for the estimation of GFR.¹³

The availability of a real-time, accurate, repeatable measure of renal excretion rate using exogenous markers under specific yet changing circumstances would represent a substantial improvement over any currently available or widely practiced method. Moreover, a method that depends solely on the renal elimination of an exogenous chemical entity would provide an absolute and continuous pharmacokinetic measurement requiring less subjective interpretation based upon age, muscle mass, blood pressure, etc. Exogenous markers such as inulin, iothalamate, ⁵¹Cr-EDTA, Gd-DTPA and

^{99m}Tc -DTPA have been used to measure GFR.¹⁴⁻¹⁶ Other markers like ^{123}I and ^{125}I labeled o-iodohippurate or ^{99m}Tc -MAG₃ are used to assess the tubular secretion process.¹⁷ Unfortunately, all of these markers suffer from various undesirable properties including the use of radioactivity, ionizing radiation, and the laborious ex-vivo handling of blood and urine samples rendering them unsuitable for real-time renal function monitoring at the bed-side. Thus, in this manuscript we report the design and synthesis of a new optimized series of renal function probe molecules and their use for the continuous monitoring of GFR by optical methods.

In general, molecules which are highly hydrophilic and small (creatinine, molecular weight = 113) to moderately sized (inulin, molecular weight ~5500) are rapidly cleared from systemic circulation by glomerular filtration.¹⁸ In addition to these properties, the ideal GFR agent would not be reabsorbed nor secreted by the renal tubule, exhibit negligible binding to plasma proteins, and have very low toxicity. In order to design optical probes that satisfy all of these requirements we were forced to strike a balance between photophysical properties, and the molecular size and hydrophilicity of the fluorophore. For example, while hydrophobic cyanine and indocyanine dyes absorb and emit optimally within the near infrared (NIR) biological window (700-900 nm), it has been difficult to render the class hydrophilic enough to function as pure GFR agents. Smaller dye molecules are more easily converted to the extremely hydrophilic species required for renal clearance, but the limited π -systems resulting from these lower molecular weight compounds generally afford one photon excitation and emission in the ultraviolet (UV). Thus, to resolve our pharmacokinetic issues in concert with obtaining the best photophysical properties possible, we have identified simple derivatives of 2,5-diaminopyrazine-3,6-dicarboxylic acid (**3**) as very low molecular weight fluorescent scaffold systems with surprisingly bright emission in the yellow-to-red region of the electromagnetic spectrum.¹⁹ SAR studies have been carried out using amide-linked variants of **3** for the simultaneous optimization of GFR pharmacokinetics and photophysical properties. We have employed a variety of hydrophilic functionality for effecting rapid renal clearance of this class of pyrazine fluorophores including carbohydrate, alcohol, amino acid and various PEG-based linker strategies. From these studies, PEG substitution has emerged as an ideal way to increase hydrophilicity and solubility, reduce toxicity, and modulate aggregation of the resulting pyrazine derivatives. We are currently investigating the variation of molecular weight and architecture (and hence hydrodynamic volume) in a series of moderately sized PEG-pyrazine derivatives. The continued hypothesis for these studies is to investigate if it is possible to obtain a probe with pure renal clearance by glomerular filtration while displaying the lowest possible volume of distribution following I.V. administration (i.e. a blood pool agent with renal clearance). This would afford an optical renal function monitoring agent with a very short terminal half-life ($t_{1/2\beta}$) for continuous or serial measurements at the bedside.

2. MATERIALS AND METHODS

2.1 Design and synthesis

Compound **3** was prepared by a modification of the method reported by Kaminsky et al.²⁰ 5-Aminouracil **1** was oxidatively cyclodimerized to afford the pyrimidinopteridine salt **2**. This compound was converted to **3** by base hydrolysis at 170 °C in a Parr apparatus or by microwave heating at the same temperature. While compound **3**, itself, is unsuitable for development as a renal function candidate due to extreme insolubility, it is an excellent scaffold for further synthetic elaboration. A small number of very lipophilic amide analogues of **3** have been previously prepared for use in solid state fluorescence studies.²¹ These reported molecules are very lipophilic and also highly water insoluble. Thus, we have designed and synthesized a number of hydrophilic amides of compound **3** for use as renal function candidates (Chart 1). Standard peptide coupling using the EDC-HOBt methodology afforded a range of bis-secondary and tertiary amides in good yield. Compounds were purified by flash chromatography (Merck 230-400mesh SiO₂) or by reversed-phase medium pressure LC (LiChroprep RP-18 Lobar (B) 25 x 310 mm – EMD chemicals 40-63 μm , ~70 g, 0.1% TFA-ACN gradients). In all cases >95% purity was achieved for animal testing. Compound **4** required a final Boc deprotection step using TFA to form compound **5**. In summary, compounds **5-9** were prepared to generate hydrophilic soluble derivatives of **3** with charges varying from cationic to neutral to anionic.

In considering how to further modify our pyrazine based systems beyond simple peptide-amide derivatives we took a closer look at the gold standard renal agent inulin. The Stokes-Einstein radius of inulin is 13 Å and its solvated molecular structure is roughly that of an elongated cylinder with a length of 25 Å and a radius of 11-13 Å.²² Thus it is easy to see how the neutral yet hydrophilic inulin would be easily filtered through the glomerular epithelial pore slit diaphragm (40 x 140 Å)²³ in even though it has a molecular weight of 5500-6000. Thus there appears to be a molecular weight regime that falls between that of small molecule drugs (~500) and macromolecules (>6,000) that could provide another novel

renal agent that is freely filtered through the glomerulus but is restricted from becoming highly distributed in the tissues. Consideration of how to elaborate our pyrazine scaffold systems to accomplish this goal, led

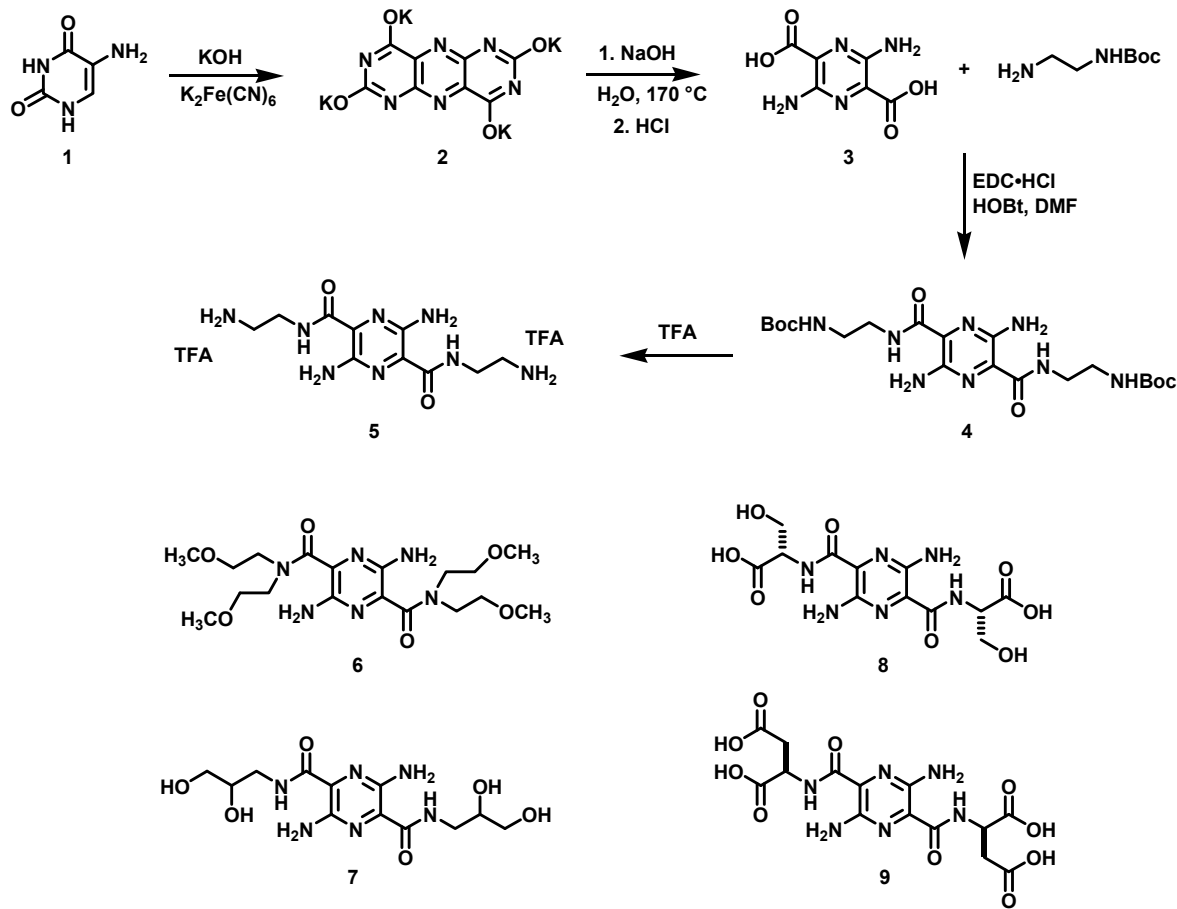


Chart 1. Synthesis of Hydrophilic Pyrazine Amide Analogues

us to consider PEG chemistry.²⁴ PEG groups are highly soluble oligomers and polymers of ethylene glycol. They are highly biocompatible, non-immunogenic and non-toxic. PEG polymers have been used primarily to modify therapeutic proteins for enhancement of their pharmacokinetic performance in vivo. PEG groups are usually of fairly high molecular weight (20-500 kDa) and may be branched or linear chains. Pegylation is known to significantly increase the apparent size (Stokes-Einstein radius or hydrodynamic volume) of the conjugated drug compound. In the case of some therapeutic proteins, the very large hydrodynamic volume of the conjugate has been shown to slow down renal clearance and prolong pharmacokinetic half-life. Ikada has studied the biodistribution of PEGs after i.v. administration and found that the terminal half-life in the circulation extended from 18 min to 1 day as the PEG molecular weight increased from 6,000 to 190,000.²⁵ We were intrigued by the lower end of this range as an 18 min terminal half-life would be quite acceptable for a renal function agent. Lower molecular weight PEG chains (at least <6,000) are known to be filtered by the glomerulus and not reabsorbed by the renal tubules.²⁵ Thus we decided to prepare a series of pegylated pyrazine conjugates for the next phase of SAR studies.

As depicted in Chart 2, intermediate **5** was acylated under standard bioconjugation conditions with a series of PEG active esters²⁶ to provide a set of compounds **11a-c** with increasing PEG lengths of from 16.4-44.9 Å. Compounds **11a-c** were purified by reversed phase LC using medium pressure conditions as described above. Compound **13** was prepared by direct coupling of **3** with 24-mer PEG amine²⁶ **12** and purified by reversed phase HPLC using a Waters Autopurification system (XBridge Prep C18, 5µm, 30 x 150 mm, 0.1% TFA-ACN gradient). Compound **15**, with a rigidified urea linkage per PEG arm was prepared from the PEG active carbamate **14** and intermediate **5**. Compound **16**, with two rigidified urea linkages per PEG arm was prepared iteratively from the corresponding PEG active carbamates using standard

coupling and deprotection chemistry. Both compounds **15** and **16** were purified by reversed phase HPLC as described above.

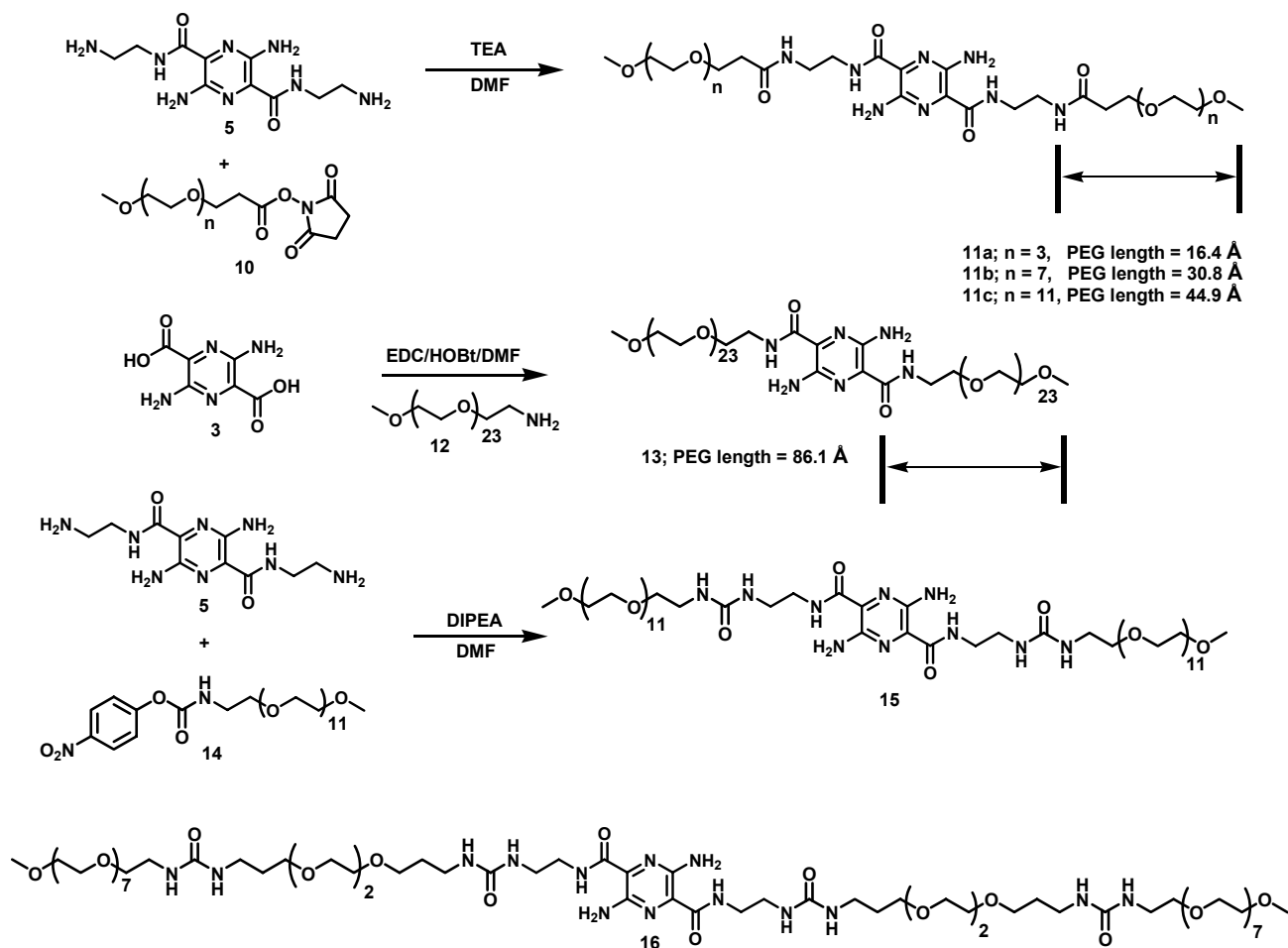


Chart 2. Synthesis of Representative Pyrazine PEG Analogues

2.2 *In vitro* characterization of compounds

The photophysical properties and plasma protein binding were determined for each compound studied. In general, each compound was dissolved in PBS buffer to form a 2 mM stock solution. The UV absorbance properties were determined on a 100 μM solution in PBS using an UV-3101PC UV-Vis-NIR Scanning spectrophotometer system from Shimadzu. The fluorescence properties (λ_{ex} , λ_{em} , and CPS at λ_{em}) were determined on a 100 nM solution in PBS using a Fluorolog-3 spectrofluorometer system from Jobin Yvon Horiba. The percent plasma protein binding was determined on a 20 μM compound solution in rat plasma incubated at 37 °C for one hour. The separation of free from bound was made using an Amicon Centrifree YM-30 device (Regenerated Cellulose 30,000 MWCO) and a Z400K Refrigerated Universal Centrifuge from Hermle. The concentration of protein-free was determined via HPLC analysis using a set of external calibration standards and fluorescence detection.

2.3 Invasive pharmacokinetic studies

Male Sprague-Dawley rats (330-380 g) were anesthetized by Inactin (I.P.). Rats were surgically instrumented with a trachea tube (PE-190) to facilitate breathing and femoral artery and vein catheters (PE-50 filled with 20 units/mL heparinized saline) for blood sampling and drug administration respectively. After administration of 1 ml of a 2 mM solution of agent, approximately 200 μL blood was sampled and placed into a heparinized tube (Microtainer Brand Tube

w/ Lithium Heparin, BD 365971) at 0, 1, 6, 12, 18, 30, 45, 60, 90, 120, 150, 180 minutes. The concentration of compound in each centrifuged plasma sample was determined via HPLC analysis using a set of external calibration standards and fluorescence detection. The resulting pharmacokinetic parameters of the compound were analyzed using WinNonLin pharmacokinetic modeling software (Pharsight, Mountain View, CA).

2.4 Non-invasive optical pharmacokinetic studies

Male Sprague-Dawley rats (330-380 g) were anesthetized by Inactin (I.P.) or 2% Isoflurane gas anesthesia delivered by a small rodent gas anesthesia machine (RC2, Vetequip, Pleasanton, CA). The animals were placed on a heated board where temperature was maintained between 36-38 °C. One ear lobe was glued flat to a glass slide positioned approximately 4mm beneath a fiber optic bundle for recording fluorescence from a test compound passing through the ear. After a 100 second baseline recording, 1ml of a 2mM solution was injected into the tail-vein of the rat and the fluorescence signal corresponding to plasma and tissue distribution and subsequent renal clearance of the compound was monitored at the ear. The pharmacokinetic parameters of the compounds were analyzed using WinNonLin pharmacokinetic modeling software (Pharsight, Mountain View, CA).

2.5 Urine elimination studies

Rat urine elimination studies were conducted by tail vein injection of 1mL of a 2 mM solution of the test compound with subsequent collection of urine at the time points of 1, 2, 4, 6, and 24 hours post injection. The metabolic cages were washed with water to maximize the recovery of urine discharged at each time point. Quantitation of each compound in urine was performed via HPLC analysis using a set of external calibration standards and fluorescence detection. The percent recovery of compound in urine at each time point was calculated based on the balance of mass.

2.6 Probenecid inhibition studies

Six female Sprague-Dawley rats were purchased from Charles River (Indianaapolis, IN) with a cannulae surgically placed in the femoral artery. Probenecid (Sigma-Aldrich; St. Louis, MO) 35 mg/kg (and 70 mg/kg) was dosed via the femoral artery cannula to three of the rats. Ten minutes post-injection of probenecid these same rats received compound **11c** (1 mL of 1 mM) via the lateral tail vein under conscious restraint. The remaining three rats received only **11c**. Once **11c** was administered, blood samples (~0.25 mL) were taken at 5, 15, 30, 45, 60, 90, 120, and 180 minute via the femoral artery catheter. Blood was collected into microfuge tubes containing 5 µl of 1000 U/ml heparin to prevent clotting. Blood samples were spun to collect plasma and the amount of **11c** in each plasma sample was determined by HPLC analysis using a set of external calibration standards and fluorescence detection.. The weight of the rat, the µg/mL of each plasma sample and the total µg/mL injected was entered into a PK Solutions 2.0 (Summit Research Services; Montrose, CO) software package which calculated clearance (mL/min).

2.7 Uranyl acetate-induced acute renal impairment

Sprague-Dawley rats were given 5 mg/kg uranyl acetate via the lateral tail vein under conscious restraint. The following day the rats were anesthetized with Inactin (100 mg/kg; ip) and a trachea tube was inserted to facilitate breathing. The rats were placed in the lateral position and the dorsal side of the left ear was glued to a microscope slide that was taped to a flat heating pad on the table top. An optical probe was positioned perpendicular to the ear and approximately 2 mm from the surface of the ventral side of the ear. An infusion set was placed in the lateral tail vein to inject the optical compound (1 mL of 2 mM).

2.8 Optical monitoring apparatus and protocol

A schematic of the apparatus for non-invasive *in vivo* detection of fluorescence is shown in Chart 3. A nominal 445 nm solid state laser source was employed (Power Technology model LDCU12/6619). The laser source was directed into one leg of a silica bifurcated fiber optic bundle (Oriel #77565). The common end of this bifurcated bundle was placed approximately 2 mm from the rat ear. The second leg of the bifurcated fiber optic bundle was fitted with a collimating beam probe (Oriel #77644). A long pass filter (Semrock LP02-488RS-25) and narrow band interference filter (Semrock FF01-560/25-25) were placed in front of a photomultiplier tube (Hamamatsu photosensor module H7827-001).

Lock-in detection was employed. A chopper (Stanford Research Systems model SR540) was placed after the laser and before the launch into the bifurcated cable. The output of the photosensor was connected to a lock-in amplifier (Stanford Research Systems model SR830) The lock-in output was digitized (National Instruments NI-USB-6211) and the digitized data was acquired by computer using LabVIEW® data acquisition software.

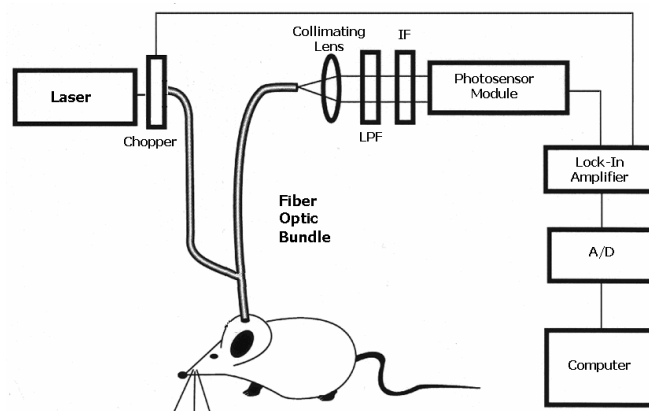


Chart 3. Apparatus for non-invasive *in vivo* detection of fluorescence

3. RESULTS AND DISCUSSION

3.1 Protein binding, photophysical properties and urine elimination studies

Protein binding and photophysical properties were determined for all compounds prior to testing in animals. In addition, new compound classes were profiled for urinary elimination prior to conducting optical monitoring and invasive PK experiments. Amide/peptide analogues **5-9** were prepared to test the effect of a varying degree of ionic charge on urinary elimination rate (glomerular filtration mechanism). The compounds provide a nice range of molecular charge types; tetra-anionic **9**, di-anionic **8**, neutral with non-protic solubilization **6**, neutral with protic solubilization **7**, and dicationic **5**. The neutral and anionic compounds were eliminated significantly by 4 hours while the cationic molecule **5** was not. This is not a surprise as it is known that cationic species can bind to various anionic phospholipid membrane structures *in vivo* and therefore decrease elimination rate.²⁷ Compound **5** was also the only compound to show significant serum protein binding. Dianion **8** was the best performer in the group with nearly 80% in the urine at the 4 hour time point. These data along with photophysical properties are presented in Table 1.

Table 1. Initial screening of pyrazine-based renal function candidates

Compound Charge or MW	Protein Binding	(2h) Urine Elimination	(4h) Urine Elimination	PPP
5, Di-Cation	20%	15%	17%	$\lambda_{ex} = 449 \text{ nm}$ $\lambda_{em} = 562 \text{ nm}$
6, Neutral	0%	39%	57%	$\lambda_{ex} = 394 \text{ nm}$ $\lambda_{em} = 550 \text{ nm}$
7, Neutral	2%	60%	61%	$\lambda_{ex} = 432 \text{ nm}$ $\lambda_{em} = 558 \text{ nm}$
8, Dianion	0%	73%	80%	$\lambda_{ex} = 449 \text{ nm}$ $\lambda_{em} = 559 \text{ nm}$
9, Tetra-anion	0%	53%	57%	$\lambda_{ex} = 449 \text{ nm}$ $\lambda_{em} = 558 \text{ nm}$

All PEG derivatives **11a-c**, **13**, **15** and **16** show no plasma protein binding and typical excitation and emission for the 1,5-diaminopyrazine-3,6-pyrazine diamide core unit at 450 nm and 560 nm respectively. As the PEG length, molecular weight and hence hydrodynamic volume were increased through the series **11a-c**, we observed a corresponding increase in renal excretion with compound **11c** showing 90% in the urine after 1 hour (Chart 4). Dosing compound **11c** with and without the organic anion transport inhibitor probenecid¹⁸ showed no difference in renal excretion suggesting there is no secretion or reabsorption occurring in the renal tubules (i.e. elimination is occurring exclusively by glomerular filtration).

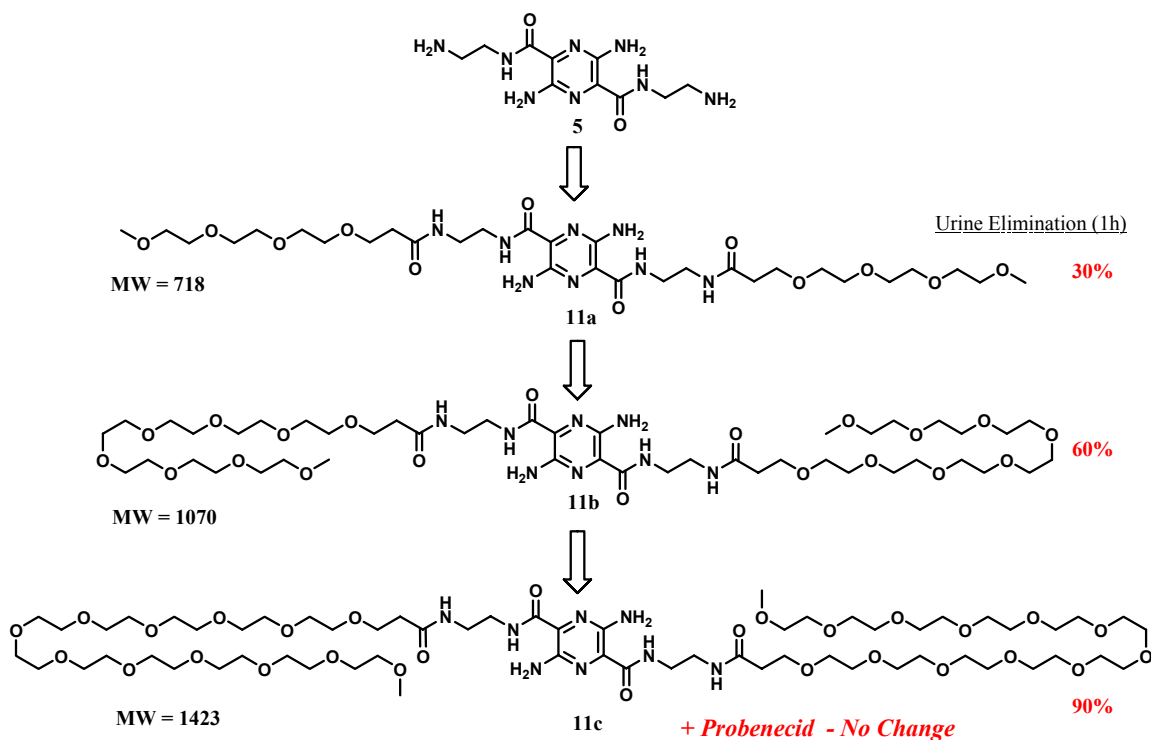


Chart 4. Increasing renal excretion with increasing PEG length.

3.2 Optical monitoring of renal elimination

Test animals were evaluated for renal function by optical monitoring methods described in section 2.8. All of the anionic and neutral compounds in Table 1 displayed a biphasic elimination profile indicating that they distribute freely from the blood into the interstitial space and thus conform to at least a two compartment pharmacokinetic model. The elimination profiles for compound **8** ($n = 3$) in animals with normal renal function are represented on the plot in Chart 5 as the lower yellow, purple and teal curves grouped together (labeled normal renal function). To further test the optical method, acute renal injury was induced by i.v. injection of uranyl acetate (5 mg/kg of body wt).²⁸ The day following injection of uranyl acetate, animals were evaluated for renal function again using compound **8**. The cyan curve represents significantly lower GFR consistent with moderately impaired renal function. After 2 days, the animals were reevaluated by the optical monitoring method again using compound **8**. The dark blue curve represents a state of highly impaired renal function and potentially the onset of renal failure.

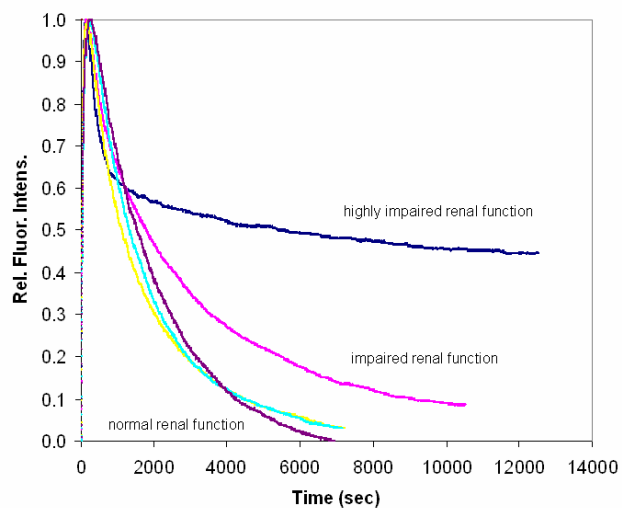


Chart 5. Non-invasive monitoring of renal function

3.3 Invasive pharmacokinetic analysis

The pharmacokinetic profiles of compounds **8**, **11c**, **15**, **16** and iothalamate are presented in Table 2. The pegylated compounds from this group **11c**, **15** and **16** are essentially equivalent to iothalamate with regard to clearance indicating that they are indeed GFR agents. Although not statistically significant, the small dianion **8** consistently shows a trend toward slower clearance. This molecule, along with other amino acid derived analogues, may be substrates for the organic anion transporter(s) (OATs) in the renal tubules. To fully understand the clearance behavior of these compounds, future work will involve probenecid competition experiments. A trend toward lower volume of distribution (V_d) and hence shorter terminal half-lives ($T_{1/2\beta}$) are also observed with with pegylated compounds. This reinforces the theory that pegylation strategies can be used minimize partitioning into the interstitium while maintaining rapid renal clearance. Future studies will involve increasing the PEG molecular weight with differing architectures to study the effect of varying hydrodynamic volume on tissue distribution.

Table 2. Pharmacokinetic profiles of renal function agents

Compound	V_d (mL/kg)	Clearance (mL/min kg)	$T_{1/2\beta}$ (min)
8	267 ± 18.5	7.32 ± 0.42	29.5 ± 3.78
11c	202 ± 2.28	9.75 ± 1.58	19.8 ± 3.73
15	188 ± 13.1	7.95 ± 0.18	21.6 ± 0.96
16	191 ± 8.46	8.77 ± 0.26	18.8 ± 0.82
Iothalamate	300 ± 29.1	8.20 ± 1.36	32.6 ± 8.74

3.4 Correlation of invasive plasma PK with optical clearance data

Time course data from an invasive plasma PK experiment and from non-invasive optical monitoring experiments have been used to correlate in vivo fluorescence response with plasma concentration in micrograms per mL. By plotting the average relative fluorescence unit response for 3 optical clearance runs versus concentration values from an invasive PK experiment for each time point an excellent correlation was demonstrated with compound **15** as shown in Chart 6. These

results clearly show that PK parameters can be determined from the optical clearance data for these compounds. *Thus GFR can be accurately obtained from the pharmacokinetic clearance value derived from direct analysis of the non-invasive optical monitoring data.*

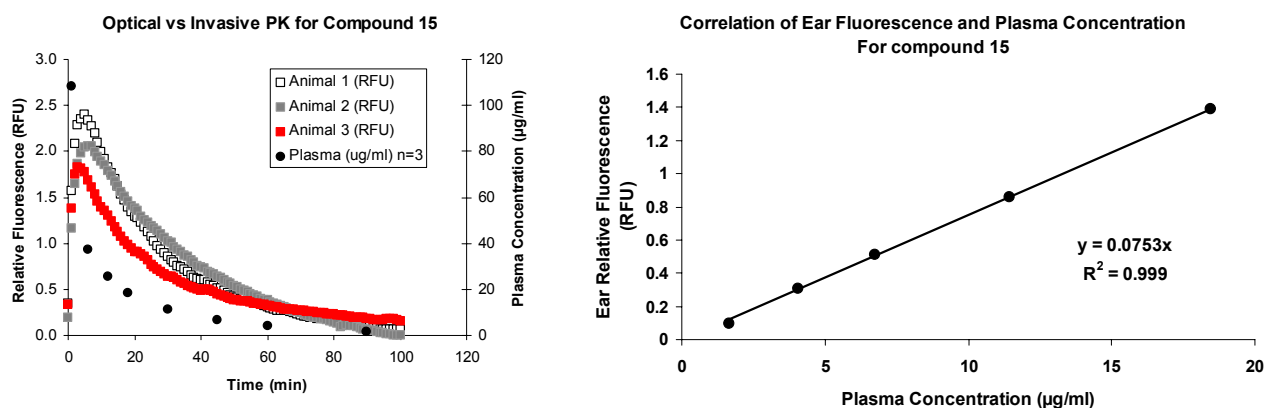


Chart 6. Correlation of in vivo fluorescence with actual plasma concentration for compound 15.

4. CONCLUSIONS

The feasibility of continuously monitoring renal function and providing an accurate real-time measure of GFR by optical methods has been demonstrated. A new class of pegylated pyrazine optical probes has been developed. Representative candidates from this class are being optimized for rapid clearance and for potential use as blood pool renal function probes. The first of these new optical probe molecules, reported herein, have been characterized for photophysical properties, protein binding, urine elimination, invasive plasma pharmacokinetics and in vivo optical monitoring performance. We have demonstrated that the invasive pharmacokinetic profile correlates extremely well with the optical monitoring data and that this data can be used to determine GFR. Future work will include continued SAR studies for further optimization of pharmacokinetics. In addition, we will continue to extend the chemistry for the preparation of new pyrazine analogues which absorb and emit at longer wavelengths.

5. ACKNOWLEDGEMENTS

The authors would like to thank Professor Thomas Dowling Pharm.D., Ph.D., University of Maryland; Dr. Carlos A. Rabito M.D., Massachusetts General Hospital; and Dr. Richard J. Solomon M.D., University of Vermont and Joseph V. Nally Jr. M.D. Dept. of Nephrology, Cleveland Clinic for valuable discussions during the course of this research.

REFERENCES

- ¹ C.A. Rabito, L.S.T. Fang, and A.C. Waltman, "Renal function in patients at risk with contrast material-induced acute renal failure: Noninvasive real-time monitoring," *Radiology* **1993**, *186*, 851-854.
- ² N.L. Tilney, and J.M. Lazarus, "Acute renal failure in surgical patients: Causes, clinical patterns, and care," *Surgical Clinics of North America* **1983**, *63*, 357-377.
- ³ B.E. VanZee, W.E. Hoy, and J.R. Jaenike, "Renal injury associated with intravenous pyelography in non-diabetic and diabetic patients," *Annals of Internal Medicine* **1978**, *89*, 51-54.
- ⁴ S. Lundqvist, G. Edbom, S. Groth, U. Stendahl and S.-O. Hietala, "Iohexol clearance for renal function measurement in gynecologic cancer patients," *Acta Radiologica* **1996**, *37*, 582-586.
- ⁵ P. Guesry, L. Kaufman, S. Orloff, J.A. Nelson, S. Swann, and M. Holliday, "Measurement of glomerular filtration rate by fluorescent excitation of non-radioactive meglumine iohalamate," *Clinical Nephrology* **1975**, *3*, 134-138.
- ⁶ C.C. Baker, L. Oppenheimer, and B. Stephens, "Epidemiology of trauma deaths," *American Journal of Surgery* **1980**, *140*, 144-150.
- ⁷ R.G. Lobenhoffer, and M. Grotz, "Treatment results of patients with multiple trauma: An analysis of 3406 cases treated between 1972 and 1991 at a German level I trauma center," *Journal of Trauma* **1995**, *38*, 70-77.
- ⁸ J. Coalson, "Pathology of sepsis, septic shock, and multiple organ failure," in *New Horizons: Multiple Organ Failure*, D.J Bihari and F.B. Cerra, Eds., pp 27-59, Society of Critical Care Medicine, Fullerton, CA, 1986.
- ⁹ F.B. Cerra, "Multiple organ failure syndrome," in *New Horizons: Multiple Organ Failure*, D.J Bihari and F.B. Cerra, Eds., pp 1-24, Society of Critical Care Medicine, Fullerton, CA, 1989.
- ¹⁰ P.D. Dollan, E.L. Alpen, and G.B. Theil, "A clinical appraisal of the plasma concentration and endogenous clearance of creatinine," *American Journal of Medicine* **1962**, *32*, 65-79.
- ¹¹ F.W. Dodge, B.L. Travis, and C.N. Daeschner, "Comparison of endogenous creatinine clearance with inulin clearance," *Am. J. Dis. Child.* **1967**, *113*, 683-692.
- ¹² J. Brochner-Mortensen, J. Giese, N. Rossing, "Renal inulin clearance versus total plasma clearance of ⁵¹Cr-EDTA," *Scand. J. Clin. Lab. Invest.* **1969**, *23*, 301-303.
- ¹³ C. White, A. Akbari, N. Hussain, L. Dinh, G. Filler, N. Lepage, and G. Knoll, "Estimating glomerular filtration rate in kidney transplantation: A comparison between serum creatinine and cystatin C-based methods," *J. Am. Soc. Nephrol.* **2005**, *16*, 3763-3770 and references cited therein.
- ¹⁴ P.L. Choyke, H.A. Austin, J.A. Frank, "Hydrated clearance of gadolinium-DTPA as a measurement of glomerular filtration rate," *Kidney International* **1992**, *41*, 1595-1598.
- ¹⁵ M.F. Tweedle, X. Zhang, M. Fernandez, P. Wedeking, A.D. Nunn, and H.W. Strauss, "A noninvasive method for monitoring renal status at the bedside," *Invest. Radiol.* **1997**, *32*, 802-805.
- ¹⁶ N. Lewis, R. Kerr, C. Van Buren, "Comparative evaluation of urographic contrast media, inulin, and ^{99m}Tc-DTPA clearance methods for determination of glomerular filtration rate in clinical transplantation," *Transplantation* **1989**, *48*, 790-796.
- ¹⁷ R. Muller-Suur, C. Muller-Suur, "Glomerular filtration and tubular secretion of MAG₃ in rat kidney," *Journal of Nuclear Medicine* **1989**, *30*, 1986-1991.
- ¹⁸ F. Roch-Ramel and M.E. De Broe, Chapter 2, "Renal handling of drugs and xenobiotics," in *Clinical Nephrotoxins: Renal Injury from Drugs and Chemicals*, M.E. De Broe, G. Porter, W. Bennett, G. Verpooten Eds., pp 21-46, Kluwer Academic Publishers, Dordrecht, The Netherlands, 2003.
- ¹⁹ K. Shirai, A. Yanagisawa, H. Takahashi, K. Fukunishi, M. Matsuoka, "Syntheses and fluorescent properties of 2,5-diamino-3,6-dicyanopyrazine dyes," *Dyes and Pigments* **1998**, *39*, 49-69.
- ²⁰ D. Kaminsky, W. Lutz and S. Lazarus, "Some congeners and analogues of dipyrindamole," *J. Med Chem.* **1966**, *9*, 610-612.
- ²¹ J. Kim, S. Shin, M. Matsuoka, and K. Fukunishi, "Self-assembling of aminopyrazine fluorescent dyes and their solid state spectra, part 2," *Dyes and Pigments* **1999**, *41*, 183-191.
- ²² F. Bodega, L. Zocchi, E. Agostoni *J. Appl. Physiol.* **2000**, *89*, 2165
- ²³ (a) Deen, W.M., Lazzara, M.J., Myers, B.D. *Am J. Renal Physiol* **2001**, *281*, F579. (b) Edwards, A., Daniels, B.S., Deen, W.M. *Am. J. Physiol.- Renal Physiol.* **1999**, *276*, F892. (c) Pavenstädt, H., Kriz, W., Kretzler, M. *Physiol Rev.* **2003**, *83*, 253. (d) Ruotsalainen, V., Ljungberg, P., Wartiovaara, J., Lenkkeri, U., Kestila, M., Jalanko, H., Holmberg, C. Tryggvason, K. *PNAS*, **1999**, *96*, 7962. (e) Wartiovaara, J. Ofverstedt, L.-G., Khoshnoodi, J., Zhang, J., Mäkelä,

- E., Sandin, S., Ruotsalainen, V., Cheng, R.H., Jalanko, H., Skoglund, U., Tryggvason, K. *J. Clin. Invest.* **2004**, *114*, 1475.
- ²⁴ (a) Zalipsky, S. *Bioconjugate Chem* **1995**, *6*, 150. (b) Greenwald, R. B., Choe, Y.H., McGuire, J. Conover, C. *Adv. Drug Del. Rev.* **2003**, *55(2)*, 217.
- ²⁵ Yamaoka, T., Tabata, Y., Ikada, Y. *J. Pharm. Sci.* **1994**, *83*, 601.
- ²⁶ All pegylation reagents were monodisperse and purchased from Quanta Biodesign.
- ²⁷ (a) Thomas, P.G., Seelig, J. *Prog. Membr. Biotechnol.* **1991**, 306. (b) Hockings, P.D., Rogers, P.J. *Biochim. et Biophys. Acta, Biomembranes* **1996**, *1282(1)*, 101. (c) Schneider, K., Naujok, A., Zimmerman, H.W., *Histochem.* **1994**, *101(6)*, 455. (d) Saito, S., Murakami, Y., Seiji, M., Kamo, N. *Biochim. et Biophys. Acta, Biomembranes* **1992** *1111(2)*, 221. (e) Demura, M., Kamo, N., Kobatake, Y. *Biochim. et Biophys. Acta, Biomembranes* **1985** *820(2)*, 207.
- ²⁸ M. Sudo, N. Honda, A. Hishida, M. Nagase “Renal hemodynamics in uranyl acetate-induced acute renal failure of rabbits” *Kidney International* **1977**, *11*, 35-43.